Thermal plasticity in coral reef symbionts is mediated by oxidation of membrane lipids

Marina Botana (m.botana23@gmail.com)
Universidade de São Paulo https://orcid.org/0000-0003-2484-6660
Adriano Chaves-Filho
Universidade de São Paulo https://orcid.org/0000-0002-2321-6504
Alex Inague
Universidade de São Paulo
Arthur Guth
Universidade de São Paulo https://orcid.org/0000-0001-8388-4187
Flavia Saldanha-Corrêa
Universidade de São Paulo
Marius Muller
Federal University of Pernambuco
Paulo Sumida
Oceanographic Institute / University of Sao Paulo https://orcid.org/0000-0001-7549-4541
Sayuri Miyamoto
Universidade de São Paulo, Instituto de Química https://orcid.org/0000-0002-5714-8984
Matthias Kellermann
University of Bremen
Raymond Valentine
University of California, Davis
Marcos Yoshinaga
Instituto de Química, Universidade de São Paulo, São Paulo, SP, 05508-000, Brazil

Article

Keywords: Lipidomics, Oxidative Stress, Coral Bleaching

Posted Date: November 3rd, 2020

DOI: https://doi.org/10.21203/rs.3.rs-96835/v1

Abstract

The oxidation of polyunsaturated fatty acids (PUFA) is a common stress response across biomes with potential to trigger impairment of cell growth and reproduction. The oxidative stress theory of coral bleaching induced by global warming has been widely accepted to explain coral reef decline, but its underlying physiological mechanism remains under debate. Here we used lipidomic and population density data to examine cell cultures of three coral reef symbionts after a heat shock (sudden rise of 12 °C for 4 hours). Heat tolerance in *S. microadriaticum* and *C. goreaui* was characterized by preservation of thylakoid-derived glycolipids. Conversely, heat sensitivity in *B. minutum* was linked to elevated concentrations of oxidized PUFA esterified to glycolipids, suggesting that culture growth had ceased due to severe oxidative damage. Our findings provide a basis to further understand the role played by oxidative stress in coral bleaching and reveal novel biomarkers for the monitoring of symbiont-coral health.

Introduction

Lipid composition of energy transducing membranes (*e.g.* cytoplasmic membranes of bacteria, thylakoid membranes of chloroplasts and mitochondrial inner membranes in eukaryotic cells) is pivotal for the survival of unicellular to complex organisms[1,2] . Energy balance in living cells is highly dependent on the efficiency of lipid membranes controlling the permeability of ions and optimizing electron transport at the membrane level, which creates proton gradients enabling mechanical energy output in the form of adenosine triphosphate (ATP)[3,4]. This process is mediated by altering the membrane fluidity and viscosity that can be regulated by the length and saturation levels of fatty acid chains of different polar lipids[1,2,5].The adjustment of membrane lipids composition in response to external abiotic stressors was suggested to be universally mediated by membrane homeoviscocity[5–7], which assures optimal cellular functions and interlinks lipids with bioenergetics[1,2,4,8].

Membranes enriched in polyunsaturated fatty acids (PUFA) are more likely to be oxidized by reactive oxygen species (ROS), especially free radicals[9,10]. If not contained by the cellular antioxidant machinery (*e.g.* enzymes and carotenoids), ROS can generate lipid radicals, which might propagate membrane lipid oxidation[10–12], unbalancing proton gradients and thus disturbing the energy balance of the cell. Oxidation of energy transducing membranes by ROS and the resulting lower concentrations of PUFA are suggested to impair distinct biological and ecological processes because of energy limitation, as shown in the inhibition of plant and algal growth[13,14], coral bleaching[15–18], and human neurodegenerative diseases[19–21].

Coral bleaching is characterized by physiological impairment of the symbiosis between cnidarian hosts and their algal symbionts (Symbiodiniaceae) and/or by loss of symbionts' photosynthetic pigments[22], potentially triggered by excessive ROS generation in the symbionts and/or the host[18]. Higher temperatures lead to increased fluidity of highly unsaturated thylakoidal membranes[23] and may cause

leakage of high-energy electrons from the water splitting reaction at the photosystem II (PSII) in Symbiodiniaceae[24]. It was suggested[15,16,25] that this process leads to increased production of ROS and cell damage in the symbionts. Besides increasing temperatures, excessive light stress can also intensify the production of ROS *via* generation of singlet oxygen[26]. Symbiodiniaceae thylakoid membranes are enriched in glycolipids linked to PUFA[27]. The greater number of double bonds compared to mono (MUFA) and saturated (SFA) fatty acids in glycolipids increase their susceptibility to ROS[10]. Several studies have suggested that Symbiodiniaceae thermal tolerance and the bleaching susceptibility of their coral hosts were defined by saturation levels of the symbiont's thylakoid membrane bond fatty acids[17,28–30]. However, this possible mechanism was inferred from the analysis of bulk fatty acid composition[17,28,30] or from a limited number of lipid classes[29,31–33]. The oxidative stress theory provides a reasonable concept to explain coral bleaching leading to worldwide coral decline[34], but up to this point, a lipid-based molecular explanation of thermal stress leading to thylakoid membrane oxidative damage is still missing. Here we show a time-dependent population density and a comprehensive untargeted lipidomic analysis (*i.e.,* lipids, quinones and pigments) of a heat shock experiment (sudden rise of 12 ˚C for 4 hours) with three different species of coral reef symbionts: *Symbiodinium microadriaticum*, *Breviolum minutum* and *Cladocopium. goreaui*. These species are broadly associated with coral hosts[35] and were previously reported to display distinct thermal tolerances[36,37] Our detailed monitoring of lipid molecular species enabled us to identify biomarkers associated with physiological acclimation strategies regarding extreme heat stress and evaluate whether the cellular damage caused by heat stress was linked to membrane lipid oxidation.

Results

A comprehensive untargeted lipidomic assessment was performed under standard culture conditions (22 ˚C; see methods section for details) to establish a baseline for the three Symbiodiniaceae species: *S. microadriaticum* (ITS2 type A1), *B. minutum* (B1) and *C. goreaui* (C1). A total of 276 compounds were identified and sorted into seven classes (*i.e.* pigments, membrane lipids as glycolipids, aminolipids, phospholipids and shingolipids; storage lipids and others) (Table 1; Fig. S1), to differentiate their presence among distinct cell compartments. The most significant difference in abundance of lipid classes among the three species was observed in the concentration of membrane lipids (ML) (1 way - ANOVA $F_{ssp.} = 51.22$; $p < 0.01$; Table S2) and their esterified fatty acids, which was up to 40% lower in *B. minutum* than in the other two species (Fig. 1a and b). Most of the lipid compounds (75 out of 86) that significantly differed among the three species were ML components (Fig. S2). Of these 75 compounds, 43 of them were esterified to omega-3 fatty acids, either octadecatrienoic acid (18:4n-3), octadecapentaenoic acid (18:5n-3) or docosahexaenoic acid (DHA; 22:6n-3). Glycolipids were predominantly linked to 18:4 and 18:5, whereas phosphatidylcholine (PC) and 1,2-diacylglyceryl-3-(O-carboxyhydroxymethylcholine (DGCC) were mostly linked to DHA (Table S1). The amounts of membrane bond oxidized PUFA (oxy-PUFA) did not differ significantly among the three species at baseline (Fig.1c).

To assess the influence of heat shock on population density, cultures were sampled over time for both heat shock and control groups of each symbiont. Biomass sampling for lipidomics was performed immediately after the four-hour long heat shock (T_4), then 24 hours later (T_{28}) and finally at the end of the experiment at 240 hours (T_{244}). Even though the control of *S. microadriaticum* had low population density number at T_{244}, no significant differences among the growing control cultures of the three species and the heat shock samples of *C. goreaui* were noticed (Table S3). On the other hand, heat shock samples of both *S. microadriaticum* and *B. minutum* showed an initial reduction to about half of their population, compared to control at T_4, thus their growth curves were significantly affected (ANCOVA $F_{HS\ [Spp]} = 26.29$; $p < 0.01$; Table S3) (Fig. 2). The only symbiont that fully ceased growth was *B. minutum*, indicated by the constant decline in its population density after heat shock (Fig. 2).

Overall alterations in lipidome profiles after heat shock

Thermal susceptibility was defined by changes in the population densities of each symbiont and by the intensity of ML remodeling, where the largest differences, those with ANOSIM R ($p < 0.01$) values approaching 1, can be visualized using the multidimensional scaling plot (MDS) (Fig. 3a). *Breviolum minutum* drastically changed its membrane lipidome (R = 0.75) with no recovery at 24 (T_{28}) nor even 240 (T_{244}) hours after heat shock (Fig. 3a), which suggest irreversibly damaged to its cells and/or cell death at T_{244}. *Symbiodinium microadriaticum* was an intermediate heat tolerant (R = 0.73) and *C. goreaui* was the most heat tolerant symbiont (R = 0.68). Differences among treatments of both *S. microadriaticum* and *C. goreaui* were within 30 Bray-Curtis similarity indexes, independent of heat shock treatment at all monitored times. The same similarity was shared only by the control of *B. minutum* (*c.f.* Fig. 3a). Glycolipids, plastoquinone and pigments, together with cardiolipin, PC and the total sum of oxy-PUFA esterified to glycolipids and DGCC were the ML classes that exhibited most variation among Symbiodiniaceae after heat shock according to principal component analysis (PCA; Fig. 3b). The greater distancing of heat shock treated samples of *B. minutum* indicated in both PCA and MDS (Fig. 3) also suggests that this heat sensitive symbiont suffered the greatest lipidome alterations. DGCC, cholesterol and other membrane components were less robust in explaining heat shock induced lipidome alterations in the Symbiodiniaceae species (cf. Fig. 3b, detailed on Table S1).

Alterations in the heat sensitive symbiont *B. minutum*

The concentration of glycolipids in heat shock samples of *B. minutum* was 77% lower than the control sample at T_4 (3-way ANOVA $F_{HS.\ [Spp.]} = 11.76$; $p < 0.01$; Table S4 and 2-way ANOVA $F_{HS} = 13.46$; $p < 0.01$; Table S5) and such variation may be explained by the reduction of PUFA linked to glycolipids ($F_{HS.\ [Spp.]} = 21.44$; $p < 0.01$; Table S4 and $F_{HS} = 26.90$; $p < 0.01$; Table S5) (Fig. 4). At $T_{244,}$ concentration of PUFA linked to glycolipids was 91% lower than control, whereas the concentration of oxy-PUFA linked to glycolipids increased by 20 times compare to the control sample ($F_{Ti.\ [Spp.]} = 8.88$; $p < 0.01$; Table S4 and $F_{Ti} = 17.57$; $p < 0.01$; Table S5). MGDG (18:4/18:5-OH) and DGDG (18:4/18:5-OH) were among the top 20 most relevant altered lipids comparing heat shock and control samples at T_{244} (Table S6). Their

concentrations increased by 1.47 and 1.12 pg, respectively, whereas concentrations of their precursors (MGDG (18:4/18:5) and DGDG (18:4/18:5) dropped to above half at T_4 and did not recover at T_{244} (Table S6). Lysolipids ($F_{HS.\ [Spp.]} = 9.09$; $p < 0.01$; Table S4) and free oxy-PUFA (oxylipins) ($F_{HS.\ [Spp.]} = 4.89$; $p < 0.01$; Table S4) also increased at T_{244} (Fig. 5c and d). Oxylipins derived from the oxidation of linoleic acid (LA; 18:2n-6), and docosahexaenoic acid (DHA; 22:6n-3), represented by hydroxyoctadienoic (HODE) and hydroxydocosahexaenoic (HDoHE) acids, respectively, were further investigated in oxylipidomics. The most abundant LA-derived oxylipins, independent of heat shock exposure, were 9- and 13-HODE isomers (Fig. S5). Relative percentages of 14- and 19-HDoHE isomers were higher than control only at T_{244} (Fig. S6). Concentrations of both plastoquinone ($F_{HS.\ [Spp.]} = 15.40$; $p < 0.01$; Table S4) and chlorophyll-*a* ($F_{HS.\ [Spp.]} = 13.97$; $p < 0.01$; Table S4) were reduced after heat shock (Fig. 5a and b), similarly to glycolipids. The concentrations of PC ($F_{HS.\ [Spp.]} = 34.38$; $p < 0.01$; Table S4), DGCC ($F_{HS.\ [Spp.]} = 33.61$; $p < 0.01$; Table S4) and cholesterol ($F_{HS.\ [Spp.]} = 15.47$; $p < 0.01$; Table S4) decreased after heat shock, whereas sphingolipids (*i.e.,* ceramides, phytoceramides and Hexosyl-ceramides) increased, exhibiting a more than 5-fold gain at T_{244} ($F_{HS.\ [Spp.]} = 7.49$; $p < 0.01$; Table S4 (Fig. S3). Overall, the storage lipids did not change significantly after heat shock, but the MUFA ($F_{HS} = 8.06$; $p < 0.01$; Table S5) content increased in triacylglycerols (TAG) at T_{244}.

Alterations in the heat tolerant symbionts *S. microadriaticum* and *C. goreaui*

Although *S. microadriaticum* and *C. goreaui* persisted growing after heat shock, their lipidome alterations were drastically different, except for the relative percentages of HODE and HDoHE isomers. As shown in *B. minutum*, LA-derived 9- and 13-HODEs were also the most abundant isomers in this two symbionts (Fig. S5), whereas HDoHEs proportions were similar after heat shock compared to controls (Fig. S6).

In *S. microadriaticum*, the concentrations of glycolipids (Fig.4), chlorophyll-*a*, oxylipins (Fig.5a and d), sphingolipids (Fig. S3d) and storage lipids (Fig. S4) did not change significantly. Plastoquinone, lysolipids (Fig. 5b and c), PC, DGCC and cholesterol (Fig. S3) slightly increased at either T_4, T_{244} or both. In *C. goreaui,* plastoquinone (Fig. 5b), PC and DGCC (Fig. S3) concentrations decreased similarly, whereas chlorophyll-*a* decreased at T_4, but increased at T_{244}, compared to control (Fig. 5a). Significant decrease in glycolipids concentration at T_{244} ($F_{HS} = 26.90$; $p < 0.01$; Table S5) was only validated by a 2-way ANOVA species-specific analysis representing a drop of 35% compared to the control samples. The concentration of oxy-PUFA esterified to glycolipids was uniquely lower than control at T_4 ($F_{Ti} = 27.61$; $p < 0.01$; Table S5) (Fig. 4). *Cladocopium goreaui* also had the lowest oxylipins content ($F_{Spp.} = 8.16$; $p < 0.01$; Table S4) among all symbionts, independently of heat shock (Fig.4). Lysolipids (Fig. 5c), cholesterol and sphingolipids (Fig.S3) concentrations remained unchanged. Storage lipids concentration increased in *C. goreaui* at T_{244} and the greatest change was observed for PUFA acyl chains esterified to TAG ($F_{HS.\ [Spp.]} = 6.62$; $p < 0.01$; Table S5), which were three times greater than the control samples (Fig. S4b).

Discussion

Monitoring population densities and distinct lipid molecular species in coral reef symbionts after an acute heat shock enabled us to formulate different underlying cellular mechanisms regarding heat tolerance. Our findings also highlight that cellular damage caused by heat stress was associated with oxidation of membrane lipids, particularly glycolipids that are a major structural component of thylakoid membranes[23]. The physiological strategies adopted to withstand heat shock exposure in each heat tolerant symbiont (*i.e.*, *S. microadriaticum* and *C. goreaui*) were species-specific and characterized by intensive lipidome remodeling. In contrast, the heat sensitivity in *B. minutum* was represented by ceased growth and a lipidome profile indicative of thylakoid membrane damage, characterized by the reduction in glycolipids, chlorophyll-*a* as well as the PSII electron transporter, plastoquinone. The oxidation of membrane lipids in *B. minutum* was further evidenced by an increase in the concentration of oxy-PUFA esterified to glycolipids and total amounts of lysolipids and oxylipins after heat shock. Not surprisingly, the greatest concentration of these biomarkers appeared at the end of the experiment in *B. minutum* when its population density was the lowest.

The protection of energy transducing membranes against lipid oxidation can be mediated by the efficiency of antioxidant machineries (*e.g.* antioxidant enzymes[38]). *Breviolum minutum* has been shown to have a less efficient enzymatic antioxidant machinery than *S. microadriaticum* and *C. goreaui* when exposed to heat stress[39], which is consistent with the reduction in its population density after heat shock. *Cladocopium goreaui* has been reported to present the highest levels of superoxide dismutase and peroxidases (putative antioxidant enzymes that avoid propagation of superoxide and peroxide ions, respectively) among the three investigated species[39–41]. This is consistent with our findings that revealed *C. goreaui* as the most tolerant symbiont (Fig. 2), the one with the lowest concentrations of both, oxy-PUFA esterified to MLs (Fig. 4) and oxylipins (Fig. 5d). Population density of *C. goreaui* did not change significantly after heat shock, but the concentrations of most of its MLs (except glycolipids), chlorophyll and plastoquinone were reduced when compared to control (Figs. 4 and S3). Lipidome data at T_{244} indicated that some membrane fatty acids, especially PUFA, could have been reallocated to storage lipids (Fig. S4), suggesting an energy saving strategy[21,42] and/or a mechanism of defense against oxidative stress[43] for preserving the thylakoid membranes specific glycolipids in this symbiont. *Symbiodinium microadriaticum* has been reported to have lower basal antioxidant enzyme levels than *C. goreaui*, though it can upregulate the production of antioxidant enzymes[39]. This heat tolerant symbiont also increased the concentration of some classes of MLs after exposure to high temperatures (Figs. 5 and S3). Both strategies (synthesis of antioxidants and ML) are energetically costly and might result in relocation of available energy, jeopardizing other metabolic needs such as growth, which might explain why this symbiont was still able to recover but had its population density significant lower than *C. goreaui*. The initial drop in the population density of *S. microadriaticum* after heat shock (T_4, Fig. 2) could have selected more thermal tolerant strains. However, it remains to be tested if the persistent population can keep the selected phenotypic traits after additional iteration of heat shock events, which would either suggest the selection of a certain heat resistant genotype or a phenotypic cell memory capacity. In the case of *C. goreaui,* where no significant drop in population density but an intense lipid remodeling was

observed, a preserved phenotypic memory response is more likely and could be an underlying mechanism to cope with abrupt changes in the natural environment[44,45]. For instance, the apex of heat stress during reoccurring El Niño events over the past decades has the potential to either select for certain genotypes with higher thermal tolerance or select for strains with a higher phenotypic cell memory capacity. Thus, symbionts that represent such heat resistant traits are more likely to thrive in future warmer oceans[46]. The efficiency of these phenotypic traits for the metabolic exchanges within coral hosts in the case of an established symbioses remains to be explored and this might be a crucial point to predict the success of coral reefs in the future.

We considered the effects of heat stress on MLs and its link to coral bleaching using an untargeted lipidomics approach. The same subject has been investigated over the past two decades[17,28–33] including studies that indirectly measured lipid oxidation and production of free radicals[47]. However, in the absence of analytical biomarkers of oxidative stress, we believe that some conclusions may be misleading. For example, Tchernov and colleagues (2004)[17] suggested that symbionts with higher concentrations of PUFA in thylakoid membranes were more susceptible to heat stress. However, in our study we demonstrate that heat tolerance/susceptibility in Symbiodiniaceae cannot be attributed to membrane saturation at baseline (see Fig. 1). Instead, our data revealed that thermal tolerance is linked to the capacity of maintaining membrane homeoviscocity stability by preserving the structural MLs (*e.g.* from oxidation; Fig. 3a and Fig. 4). In energy transducing membranes, higher unsaturation levels enable fast electron flow leading to high energy production[7]. However, such efficiency in energy transduction provided by highly unsaturated MLs is only possible with either an extremely constant environment or a concurrent evolution of powerful antioxidant machinery to preserve membrane PUFA against oxidation[1,2,9,10,38]. The latter was not the case for *B. minutum*. When ROS propagation cannot be contained, formation of lipid radicals leads to a chain reaction (Fig. 6). The addition of an oxygen-carbon bond in Oxy-PUFA may reorient the acyl chain, whereby it no longer remains in the membrane interior, but rather protrudes into the aqueous compartment[9]. Hydrolysis of the formed Oxy-PUFA leads to subsequent generation of lysolipids and oxylipins (Fig. 6). Higher concentration of lysolipids causes structural changes in membrane curvature and elasticity[48], which unbalances the stability of ion channels[49]. Such alterations may also cause proton leakage[50] unbalancing final energy output, which might inhibit cell growth and division due to a lack of energy (Fig. 6).

Free oxidized fatty acids (oxylipins) likely derived from PUFA oxidation[10] were here represented by C_{18} and C_{22} -n-3 fatty acids. Lipoxygenases (LOX) catalyze the addition of hydroperoxyl groups on specific positions of PUFA; thus, few types of positional isomers are formed through this synthesis pathway. Phytoplankton[51–53] and macroalgae[54] usually employ 9 and 13-LOX for oxidation of C_{18} and 12- and 6-LOX for oxidation of C_{20} derivatives. Unfortunately, LOX enzymes for HODEs and HDoHEs production in Symbiodiniaceae have never been explored. If the here identified positional isomers of HODEs and HDoHEs were mediated enzymatically remains to be tested. We detected oxidation *via* singlet oxygen[55] (12-HODE, 10-HODE and 19-HDoHE), as previously reported for plants[56,57]. The great diversity of isomers

showed in our study (see Figs. S5 and S6), lacking preferential generation of positional isomer type in the heat shock samples compared to controls, suggests lipid oxidation predominantly mediated by free radicals. Oxylipins and oxidized fatty acids esterified to MLs were present in all samples (including controls – Figs. 1c; S5 and S6), which is consistent with their pivotal role in biological systems as signaling molecules that accumulate as a function of abiotic and/or biotic stress[58,59] such as higher temperatures[14]. Oxidation-derived products in coral hosts (*e.g.,* eicosanoids, prostaglandins and aldehydes) has shown to mediate symbiont-host communication[60]; thus, symbiosis impairment might be a final consequence of the accumulation of these signaling molecules in response to stress.

The concentration of sphingolipids observed in *B. minutum* after heat shock was the highest at the end of the experiment when compared to the control samples (Figs. 2 and S3d). Accumulation of sphingolipids in response to heat stress has been reported across all life forms from unicellular bacteria and yeast to plants and mammals, as a strategy to adjust membrane fluidity and permeability[61]. Furthermore, cell death through apoptosis, such as proposed for mitochondria under ROS damage, is known to be linked to upregulation in sphingolipids such as ceramides[62,63]. These alterations accompanied by dysregulation in cholesterol homeostasis (also noticed in *B. minutum*; Fig. S3c) are molecular signatures in aging and during evolution of neurodegenerative diseases in humans (*i.e.*, Parkinson's disease[19], Alzheimer[20] and amyotrophic lateral sclerosis[21]). In the marine environment, apoptosis mediated by mitochondrial damage in cnidarian host cells was proposed to cause impairment of symbiont-host association and to promote bleaching[64]. Whenever bleaching is controlled by the symbionts or the host, thylakoid and mitochondria membranes' bioenergetics and lipidomes must be preserved to assure the success of this relationship.

Our findings indicate that the oxidation of PUFA in thylakoid membranes may explain cellular damage in Symbiodiniaceae under thermal stress and provide novel insights into the current knowledge of the oxidative stress theory of coral bleaching. We suggest that oxidation of PUFA in MLs may cause conformational alterations in energy transducing membranes, leading to energy limitation, impairment of cell growth and reproduction. This stress response is a common feature across biomes with the potential to trigger several morbidities ranging from neurodegenerative diseases in humans to worldwide coral reef decline. The biomarkers presented here have potential for the monitoring of coral health, and for improving the strategies for coral reef conservation. Lipidomics and metabolomics may be used in combination with other "omics" approaches (*i.e.,* genomics, transcriptomics and proteomics) to better understand how the genetic code is interacting with cellular physiology and expression of phenotypic traits. An improved interaction between these areas will bring new insights for understanding symbiont-coral host cellular communication, as well as better predict coral bleaching events in warmer future oceans.

Methods

Experimental setup

Symbiodiniaceae cultures (*S. microadriaticum* – ITS2 A1; *B. minutum*- B1 and *C. goreaui* – C1) were received from the University at Buffalo (NY-USA) and kept in the BMAK microalgae facility at the Instituto Oceanográfico from Universidade de São Paulo (IO-USP). The cultures of each symbiont were replicated equally into six 1L Erlenmeyer bottles (heat shock and control samples were performed in triplicates) containing sterile natural sea water with f/2 nutrient conditions[65]. Bottles were randomly distributed in a water bath maintained at 22 ºC. Sterilized temperature sensors (± 0.5 ºC) were added inside the cultures of each bottle to monitor temperature throughout the experiment. Cool fluorescent lights were used, and light availability kept constant at 80 $\mu E.m^{-2}$ s^{-1} in a 12:12 hours light: dark cycle. Initial cell number in each bottle was 500 $cells.ml^{-1}$ and population densities were monitored over time (Fig. 2) using a Neubauer counting chamber. Heat shock was administered once all cultures were in exponential growth (240 hours of cultivation). A separate water bath was used and pre-warmed to 34 ºC using electrical aquarium heaters (± 0.5 ºC). Three bottles of each symbiont (nine in total) were transferred from 22 ºC to the pre-heated water bath container where a temperature of 34 ºC was reached after 20 min (T_0). Subsequently, the 34 °C heat shock period was applied for 4 hours. Samples were immediately taken at the end of heat shock period (T_4) to evaluate short-term lipidome alterations between the heat shock and control populations. Afterwards, culture bottles were transferred back to the 22 ºC water baths. Both treatment groups were sampled again after 240 hours (T_{244}) for analyses of long-term changes in lipidomes. Additional samples were collected from the heat shock populations one day after the event (T_{28}) to describe potential rapid recovery of lipidome profiles after a return to the initial temperature. Bottles were slowly hand rotated for homogenization before sampling. No additional analysis was made to guarantee that only living cells were sampled in each culture bottles. All samplings occurred at the same time during the light phase. Samples for lipid and pigment analysis were taken with sterile pipets and subsequently filtered onto pre-combusted GF/F filters (10 min under 300 °C). Cell numbers exceed 1 million per filter and the true number of cells per filter was then calculated from the cell density in the remainder of the cultures after filtration on the sampling days.

Standards

Internal standards for sphingolipids, phospholipids and storage lipids were obtained from Avanti Polar Lipids, Inc. (Alabaster, AL. USA). They were added to each sample allowing for further identification and quantitative corrections. Description and concentration of each component are described in Table S7. Aminolipids and glycolipids as well as pigments had external calibration curves and standards were obtained from Avanti Polar Lipids, Inc. (Alabaster, AL. USA) and DHI Labs (Denmark), respectively.

Lipid extraction

Lipid extraction was performed according to an adaptation of the Bligh & Dyer (1959)[66] method. Each GF/F sample filter was macerated and homogenized in 1 mL of 10 mM phosphate buffer (pH 7.4) containing deferoxamine mesylate 100 µM. Then 800 µL of methanol and 200 µL of internal standard mix (10 $\mu g.ml^{-1}$) were added. Next, 4 mL of chloroform/ethyl acetate (4:1) were added to each mixture

and thoroughly vortexed for 1 minute. All procedures were performed on top of crushed ice to minimize evaporation of the solvents. Samples were sonicated for 20 min to enhance breakage of glycomembranes. After centrifugation (2000g for 6 min at 4 °C) the lower phase containing the total lipid extract (TLE) was transferred to a new tube and dried under N_2 gas. Dried TLE was again dissolved in 100 µL of isopropanol for analysis and the injection volume was set at 1 µL.

Lipidomic analysis and data processing

TLE was analyzed using an ESI-TOFMS (Triple TOF 6600, Sciex, Concord, US) interfaced with a high-performance LC system (UHPLC Nexera, Shimadzu, Kyoto, Japan), as described previously in Chaves-Filho et al. (2019)[21].

MS/MS data was analyzed with PeakView® and lipid molecular species were identified by an in-house manufactured Excel-based macro. Spectrums, showing fragment breaks including exact masses and retention times used for identification, are exemplified in the additional information. Pigments, plastoquinone, cholesterol, DAG, TAG and CE were fully analyzed in the positive mode. Aminolipids and glycolipis lipids were identified in the positive mode but quantified in the negative mode. All other membrane lipids and FFA were fully analyzed in the negative mode. Area of each lipid species were obtained by MS data from MultiQuant®. For quantification, the peak area of each lipid species was divided by the peak area of their corresponding internal standard (shown in detail in Table S7). Pigments, cholesterol and FFA had external calibration curves relative to LysoPC (17:0) internal standard (IS); DAG had external calibration curve relative to TAG (17:0/17:0/17:0) IS. PI, aminolipids and glycolipids had external calibration curves which were relative to PC (17:0/17:0) IS. They were injected separately following dilution curves with eleven points each based on concentration ranges described in Tables S8 and S9. Throughout the dilution curves, each point had half the concentration of the previous point and lower limits were defined based on MS inferior limit of detection. Specific correction factors were calculated as slopes from graph curves of each external standard divided by their respective above-mentioned internal standards. For these specific groups, final concentrations were obtained from the peak area ratio divided by their respective internal standard area ratio and multiplied by their respective correction factor (for details see Table S8 and S9). No external calibration was performed for plastoquinone. Its peak area was divided by the peak area of Lyso PC (17:0) because of its similarities in retention time. Therefore, plastoquinone concentration values still not precise as the other lipid compounds and they are better interpreted by comparing within samples.

Oxylipidomic analysis

TLE was spiked with the internal standard 5-HETE-d8 (100 ng) and 9-HODE-d4 (100 ng) and analyzed using an ESI-TOFMS (Triple TOF 6600, Sciex, Concord, US) interfaced with a high-performance LC system (UHPLC Nexera, Shimadzu, Kyoto, Japan). The HODE and HDoHE standards were synthesized and purified as previously described in Derogis *et al.* (2013)[67]. Samples were loaded into a BEH column (UPLC® C18 column, 1.7 µm, 2.1 mm i.d. x 100 mm) with a flow rate of 0.5 mL/min and oven temperature

at 35 °C. For RPLC, The mobile phase A consisted of acetic acid/water/acetonitrile (0.02:50:50), while mobile phase B composed of acetic acid/acetonitrile/isopropanol (0.02:50:50) for the lipid analyses performed in negative ionization mode[68]. The linear gradient during RPLC was as follows: from 0.1 to 55% B over the first 4 min, 55 to 99% B from 4-4.5 min, hold at 99% B from 4.5-6.5 min, decreased from 99 to 0.1% B from 6.5-7 min, and hold at 0.1% B from 7-10 min. The MS was operated in negative ionization mode, and the scan range set at a mass-to-charge ratio of 200-1000 Da. Data for lipid molecular species identification and quantification was obtained with the targeted product ion acquisition method. Data acquisition was performed with a period cycle time of 0.56 s with 100 ms acquisition time for the MS1 scan and 10 ms for the MS/MS scan. Data acquisition was performed using Analyst® 1.7.1 with an ion spray voltage of -4.5 kV and the cone voltage at - 80 V. The curtain gas was set at 25 psi, nebulizer and heater gases at 50 psi and interface heater at 500 °C. Specific fragments used of each oxidized lipid were manually identified using PeakView® and ChemDraw® softwares (Table S10), as previously described[67]. Identification and quantification were performed by monitoring the specific fragments of each analyte using Multiquant® software. The area of analytes was obtained by using 5 mDa as the maximum acceptable mass error. The area ratio obtained for each lipid molecular specie was calculated by dividing the peak area of the lipid by the corresponding internal standard (Table S10). The concentration of lipid species was calculated by applying the area ratio in a calibrate curve constructed for each analyte. Data are presented as relative percentages. This analysis was performed separately from lipidomics, so that data generated here are not comparable to relative percentages, neither to abundances of lipid compounds monitored through lipidomics.

Statistical analysis

All lipid compounds described in our work (276 lipid molecules) were sorted into the main lipid classes (Table S1). Differences among the lipidomes of symbionts growing at 22 ˚C (controls) were stablished before applying the heat shock considering the total sums of each lipid class. For that we used a one-way ANOVA analysis followed by Tukey's HSD ($p < 0.01$) corrected by a false discovery rate (FDR) routine using MetaboAnalyst 4.0 software[69]. A two-way analysis of covariance (ANCOVA) was performed to test for significant differences in cell density development over time between the control and heat shock groups of each species. ANCOVA used time (hours of experiment) as a covariable and Heat shock ((T) /Control (C)) nested within each species. Pairwise comparisons between heat shock and control within the same time; and heat shock over time (T_4, T_{28} and T_{244}), for each specie were tested with Tukey's HSD post-hoc test ($p < 0.01$) (JMP v8.0 statistical software).

Further analyses on lipidomic focused on 133 membrane lipids and pigments organized in their classes and performed separated from other characterized compounds (*i.e.* storage lipids, DAG and FFA). First, multidimensional scaling (MDS) and analysis of similarity (ANOSIM) (both ran with Primer 6.0[70]) were used to visualize and test the differences among heat shock and control in each species and among species. Positive pairwise R values from ANOSIM were used as indicators of the intensity of membrane lipid remodeling caused by heat shock in each Symbiodinaceae. Principal component analysis (PCA) was

used to identify the groups of membrane lipids responsible for the main differences caused by heat shock (classes detailed in Table S1). After this screening, each one of these lipid classes, together with storage lipids and oxylipins were tested for significant differences among the experimental units with a 3-way mixed ANOVA to evaluate the differences between heat shock and control among species using heat shock (HS; two levels: control and treatment) orthogonal to time (Ti; two levels: T_4 and T_{244}) and nested within each Symbiodiniaceae species (Spp.; three levels: A1, B1 and C1). A further 2-way crossed ANOVA was performed to evaluate the differences between heat shock and control individually in each species using heat shock (HS; two levels: control and treatment) orthogonal to time (Ti; two levels: T_4 and T_{244}). Pairwise comparisons were tested with Tukey's HSD test, significance threshold was set at $p < 0.01$. The same matrix of 133 membrane lipids was used for similarity percentages (SIMPER) analyses (using Primer 6.0) comparing heat shock and control of each symbiont for identification of individual lipid compounds as heat stress biomarkers. All data of parametric tests were tested for homoscedasticity and log-transformed when necessary. Data was log-transformed (except in SIMPER analyses), so that the variations in less abundant lipids are comparable to more abundant compounds.

Declarations

Acknowledgements

We thank David Valentine (Presidential Chair, Professor of Earth Science and Biology, UC Santa Barbara), Simon Davy (Professor of Marine Biology, School of Biological Sciences, Victoria University of Wellington), Miguel Mies (Research Coordinator, Instituto Coral Vivo) and Linda Waters (Post-doc fellow at Instituto Oceanográfico, Universidade de São Paulo) for reviewing the manuscript. We also thank Florence Schubotz (Research fellow, MARUM – University of Bremen) and Frederico Brandini (Professor of Biological Oceanography, Instituto Oceanográfico, Universidade de São Paulo) for kindly donating standards for our external calibration curves. This study was financed in part by the Coordenação de Aperfeiçoamento de Pessoal de Nível Superior – Brazil (CAPES) Finance Code 001. SM is supported by FAPESP (#13/07937-8) and CNPq (#424094/2016-9 and #309083/2017-6).

Contributions

M.T.B. experiment, cell density monitoring, lipidomics, data analysis and manuscript writing; A.B.C.F. analytical design, lipidomics and oxylipidomics; A.I. analytical design and lipidomics; A.Z.G. data analysis and manuscript writing; F.S.C. study design; M.N.M. data analysis and manuscript writing; P.Y.G.S. study design and project funding; S.M. analytical design, lipidomics and oxylipidomics; M.Y.K. lipidomics and study design; R.C.V. study design; M.Y.Y. lipidomics, oxylipidomics and manuscript writing. All authors provided substantial comments on the manuscript.

Ethics declaration

The authors declare no competing interests.

References

1. Valentine, R. C. & Valentine, D. L. Omega-3 fatty acids in cellular membranes: a unified concept. *Progress in Lipid Research* 43, 383–402 (2004).
2. Valentine, R. C. & Valentine, D. L. *Omega-3 Fatty Acids and the DHA Principle*. (CRC Press, 2009).
3. Daum, B., Nicastro, D., Austin, J., McIntosh, J. R. & Kühlbrandt, W. Arrangement of Photosystem II and ATP Synthase in Chloroplast Membranes of Spinach and Pea. *The Plant Cell* 22, 1299–1312 (2010).
4. Yoshinaga, M. Y., Kellermann, M. Y., Valentine, D. L. & Valentine, R. C. Phospholipids and glycolipids mediate proton containment and circulation along the surface of energy-transducing membranes. *Progress in Lipid Research* 64, 1–15 (2016).
5. Sinensky, M. Homeoviscous Adaptation—A Homeostatic Process that Regulates the Viscosity of Membrane Lipids in Escherichia coli. *PNAS* 71, 522–525 (1974).
6. Cossins, A. R. & Prosser, C. L. Evolutionary adaptation of membranes to temperature. *PNAS* 75, 2040–2043 (1978).
7. Budin, I. *et al.* Viscous control of cellular respiration by membrane lipid composition. *Science* 362, 1186–1189 (2018).
8. Kellermann, M. Y., Yoshinaga, M. Y., Valentine, R. C., Wörmer, L. & Valentine, D. L. Important roles for membrane lipids in haloarchaeal bioenergetics. *Biochimica et Biophysica Acta (BBA) - Biomembranes* 1858, 2940–2956 (2016).
9. Greenberg, M. E. *et al.* The Lipid Whisker Model of the Structure of Oxidized Cell Membranes. *J. Biol. Chem.* 283, 2385–2396 (2008).
10. Yin, H., Xu, L. & Porter, N. A. Free Radical Lipid Peroxidation: Mechanisms and Analysis. *Chem. Rev.* 111, 5944–5972 (2011).
11. Smith, W. L. & Murphy, R. C. Oxidized Lipids Formed Non-enzymatically by Reactive Oxygen Species. *J. Biol. Chem.* 283, 15513–15514 (2008).
12. Niki, E. Lipid peroxidation: Physiological levels and dual biological effects. *Free Radical Biology and Medicine* 47, 469–484 (2009).
13. Falcone, D. L., Ogas, J. P. & Sommerville, C. L. Regulation of membrane fatty acid composition by temperature in mutants of Arabidopsis with alterations in membrane lipid composition | SpringerLink. https://link.springer.com/article/10.1186/1471-2229-4-17.
14. Luo, Q. *et al.* Different Responses to Heat Shock Stress Revealed Heteromorphic Adaptation Strategy of Pyropia haitanensis (Bangiales, Rhodophyta). *PLoS ONE* 9, e94354 (2014).
15. Lesser, M. P. Oxidative stress causes coral bleaching during exposure to elevated temperatures. *Coral Reefs* 16, 187–192 (1997).
16. Lesser, M. P. OXIDATIVE STRESS IN MARINE ENVIRONMENTS: Biochemistry and Physiological Ecology. *Annu. Rev. Physiol.* 68, 253–278 (2006).

17. Tchernov, D. *et al.* Membrane lipids of symbiotic algae are diagnostic of sensitivity to thermal bleaching in corals. *Proceedings of the National Academy of Sciences* 101, 13531–13535 (2004).
18. Weis, V. M. Cellular mechanisms of Cnidarian bleaching: stress causes the collapse of symbiosis. *Journal of Experimental Biology* 211, 3059–3066 (2008).
19. Farooqui, A. A., Horrocks, L. A. & Farooqui, T. Glycerophospholipids in brain: their metabolism, incorporation into membranes, functions, and involvement in neurological disorders. *Chemistry and Physics of Lipids* 106, 1–29 (2000).
20. Cutler, R. G. *et al.* Involvement of oxidative stress-induced abnormalities in ceramide and cholesterol metabolism in brain aging and Alzheimer's disease. *PNAS* 101, 2070–2075 (2004).
21. Chaves-Filho, A. B. *et al.* Alterations in lipid metabolism of spinal cord linked to amyotrophic lateral sclerosis. *Sci Rep* 9, 11642 (2019).
22. Glynn, P. W. Coral reef bleaching: ecological perspectives. *Coral Reefs* 12, 1–17 (1993).
23. Los, D. A. & Murata, N. Membrane fluidity and its roles in the perception of environmental signals. *Biochimica et Biophysica Acta (BBA) - Biomembranes* 1666, 142–157 (2004).
24. Slavov, C. *et al.* "Super-quenching" state protects Symbiodinium from thermal stress — Implications for coral bleaching. *Biochimica et Biophysica Acta (BBA) - Bioenergetics* 1857, 840–847 (2016).
25. Goyen, S. *et al.* A molecular physiology basis for functional diversity of hydrogen peroxide production amongst Symbiodinium spp. (Dinophyceae). *Mar Biol* 164, 46 (2017).
26. Pospíšil, P. Production of Reactive Oxygen Species by Photosystem II as a Response to Light and Temperature Stress. *Front. Plant Sci.* 7, (2016).
27. Leblond, J. D. & Chapman, P. J. LIPID CLASS DISTRIBUTION OF HIGHLY UNSATURATED LONG CHAIN FATTY ACIDS IN MARINE DINOFLAGELLATES. *Journal of Phycology* 36, 1103–1108 (2000).
28. Bachok, Z., Mfilinge, P. & Tsuchiya, M. Characterization of fatty acid composition in healthy and bleached corals from Okinawa, Japan. *Coral Reefs* 25, 545–554 (2006).
29. Tolosa, I., Treignier, C., Grover, R. & Ferrier-Pagès, C. Impact of feeding and short-term temperature stress on the content and isotopic signature of fatty acids, sterols, and alcohols in the scleractinian coral Turbinaria reniformis | SpringerLink. https://link.springer.com/article/10.1007/s00338-011-0753-3.
30. Kneeland, J., Hughen, K., Cervino, J., Hauff, B. & Eglinton, T. Lipid biomarkers in Symbiodinium dinoflagellates: new indicators of thermal stress. *Coral Reefs* 32, 923–934 (2013).
31. Imbs, A. B. & Yakovleva, I. M. Dynamics of lipid and fatty acid composition of shallow-water corals under thermal stress: an experimental approach. *Coral Reefs* 31, 41–53 (2012).
32. Rosset, S. *et al.* Lipidome analysis of Symbiodiniaceae reveals possible mechanisms of heat stress tolerance in reef coral symbionts. *Coral Reefs* 38, 1241–1253 (2019).
33. Solomon, S. L. *et al.* Lipid class composition of annually bleached Caribbean corals. *Mar Biol* 167, 7 (2020).

34. Oakley, C. A. & Davy, S. K. Cell Biology of Coral Bleaching | SpringerLink. https://link.springer.com/chapter/10.1007/978-3-319-75393-5_8.
35. LaJeunesse, T. C. *et al.* Systematic Revision of Symbiodiniaceae Highlights the Antiquity and Diversity of Coral Endosymbionts. *Current Biology* 28, 2570-2580.e6 (2018).
36. Swain, T. D., Chandler, J., Backman, V. & Marcelino, L. Consensus thermotolerance ranking for 110 Symbiodinium phylotypes: an exemplar utilization of a novel iterative partial-rank aggregation tool with broad application potential. *Functional Ecology* 31, 172–183 (2017).
37. Lesser, M. P. Phylogenetic signature of light and thermal stress for the endosymbiotic dinoflagellates of corals (Family Symbiodiniaceae). *Limnol Oceanogr* 64, 1852–1863 (2019).
38. Imlay, J. A. The molecular mechanisms and physiological consequences of oxidative stress: lessons from a model bacterium. *Nat Rev Microbiol* 11, 443–454 (2013).
39. McGinty, E. S., Pieczonka, J. & Mydlarz, L. D. Variations in Reactive Oxygen Release and Antioxidant Activity in Multiple Symbiodinium Types in Response to Elevated Temperature. *Microb Ecol* 64, 1000–1007 (2012).
40. Krueger, T. *et al.* Antioxidant plasticity and thermal sensitivity in four types of *Symbiodinium* sp. *J. Phycol.* 50, 1035–1047 (2014).
41. Ladner, J. T., Barshis, D. J. & Palumbi, S. R. Protein evolution in two co-occurring types of Symbiodinium: an exploration into the genetic basis of thermal tolerance in Symbiodinium clade D. *BMC Evol Biol* 12, 217 (2012).
42. Bailey, A. P. *et al.* Antioxidant Role for Lipid Droplets in a Stem Cell Niche of Drosophila. *Cell* 163, 340–353 (2015).
43. Green, D. R. Immiscible immunity. *Science* 370, 294–295 (2020).
44. Kordes, A. *et al.* Establishment of an induced memory response in Pseudomonas aeruginosa during infection of a eukaryotic host. *ISME J* 13, 2018–2030 (2019).
45. Rescan, M., Grulois, D., Ortega-Aboud, E. & Chevin, L.-M. Phenotypic memory drives population growth and extinction risk in a noisy environment. *Nat Ecol Evol* 4, 193–201 (2020).
46. Bindoff, N. L. Changing Ocean, Marine Ecosystems, and Dependent Communities - Research Collection. https://www.research-collection.ethz.ch/handle/20.500.11850/395234.
47. Nielsen, D. A., Petrou, K. & Gates, R. D. Coral bleaching from a single cell perspective. *ISME J* 12, 1558–1567 (2018).
48. Fuller, N. & Rand, R. P. The Influence of Lysolipids on the Spontaneous Curvature and Bending Elasticity of Phospholipid Membranes. *Biophysical Journal* 81, 243–254 (2001).
49. McMahon, H. T. & Gallop, J. L. Membrane curvature and mechanisms of dynamic cell membrane remodelling. *Nature* 438, 590–596 (2005).
50. Bacellar, I. O. L. & Baptista, M. S. Mechanisms of Photosensitized Lipid Oxidation and Membrane Permeabilization. *ACS Omega* 4, 21636–21646 (2019).

51. Gerwick, W. H. Structure and biosynthesis of marine algal oxylipins. *Biochimica et Biophysica Acta (BBA) - Lipids and Lipid Metabolism* 1211, 243–255 (1994).
52. Russo, E. *et al.* Density-dependent oxylipin production in natural diatom communities: possible implications for plankton dynamics. *ISME J* 14, 164–177 (2020).
53. Ruocco, N. *et al.* Lipoxygenase Pathways in Diatoms: Occurrence and Correlation with Grazer Toxicity in Four Benthic Species. *Marine Drugs* 18, 66 (2020).
54. Chen, H. *et al.* 1-Octen-3-ol, a self-stimulating oxylipin messenger, can prime and induce defense of marine alga. *BMC Plant Biol* 19, 1–16 (2019).
55. Mascio, P. D. *et al.* Singlet Molecular Oxygen Reactions with Nucleic Acids, Lipids, and Proteins. *Chemical Reviews* (2019) doi:10.1021/acs.chemrev.8b00554.
56. Triantaphylidès, C. *et al.* Singlet Oxygen Is the Major Reactive Oxygen Species Involved in Photooxidative Damage to Plants. *Plant Physiology* 148, 960–968 (2008).
57. Oenel, A. *et al.* Enzymatic and Non-Enzymatic Mechanisms Contribute to Lipid Oxidation During Seed Aging. *Plant Cell Physiol* 58, 925–933 (2017).
58. Vu, H. S. *et al.* Direct Infusion Mass Spectrometry of Oxylipin-Containing Arabidopsis Membrane Lipids Reveals Varied Patterns in Different Stress Responses. *Plant Physiology* 158, 324–339 (2012).
59. Collins, J. R., Edwards, B. R., Fredricks, H. F. & Mooy, B. A. S. V. LOBSTAHS: An Adduct-Based Lipidomics Strategy for Discovery and Identification of Oxidative Stress Biomarkers. https://pubs.acs.org/doi/abs/10.1021/acs.analchem.6b01260 (2016) doi:10.1021/acs.analchem.6b01260.
60. Matthews, J. L. *et al.* Optimal nutrient exchange and immune responses operate in partner specificity in the cnidarian-dinoflagellate symbiosis. *PNAS* 114, 13194–13199 (2017).
61. Fabri, J. H. T. M. The dynamics and role of sphingolipids in eukaryotic organisms upon thermal adaptation. *Progress in Lipid Research* 80, 101063 (2020).
62. Ariga, T., Jarvis, W. D. & Yu, R. K. Role of sphingolipid-mediated cell death in neurodegenerative diseases. *J. Lipid Res.* 39, 1–16 (1998).
63. Hannun, Y. A. & Obeid, L. M. Principles of bioactive lipid signalling: lessons from sphingolipids. *Nat Rev Mol Cell Biol* 9, 139–150 (2008).
64. Dunn, S. R., Pernice, M., Green, K., Hoegh-Guldberg, O. & Dove, S. G. Thermal Stress Promotes Host Mitochondrial Degradation in Symbiotic Cnidarians: Are the Batteries of the Reef Going to Run Out? *PLOS ONE* 7, e39024 (2012).
65. Guillard, R. R. L. & Ryther, J. H. STUDIES OF MARINE PLANKTONIC DIATOMS: I. CYCLOTELLA NANA HUSTEDT, AND DETONULA CONFERVACEA (CLEVE) GRAN. *Canadian Journal of Microbiology* (2011) doi:10.1139/m62-029.
66. Bligh, E. G. & Dyer, W. J. A rapid method for lipid extraction and purification. https://cdnsciencepub.com/doi/abs/10.1139/o59-099.

67. Derogis, P. B. M. C. *et al.* The Development of a Specific and Sensitive LC-MS-Based Method for the Detection and Quantification of Hydroperoxy- and Hydroxydocosahexaenoic Acids as a Tool for Lipidomic Analysis. *PLOS ONE* 8, e77561 (2013).
68. Wang, Y. Comprehensive ultra-performance liquid chromatographic separation and mass spectrometric analysis of eicosanoid metabolites in human samples. *Journal of Chromatography A* 1359, 60–69 (2014).
69. Chong, J., Wishart, D. S. & Xia, J. Using MetaboAnalyst 4.0 for Comprehensive and Integrative Metabolomics Data Analysis - Chong - 2019 - Current Protocols in Bioinformatics - Wiley Online Library. https://currentprotocols.onlinelibrary.wiley.com/doi/abs/10.1002/cpbi.86.
70. Clarke, L. J., Soubrier, J., Weyrich, L. S. & Cooper, A. Environmental metabarcodes for insects: in silico PCR reveals potential for taxonomic bias. *Molecular Ecology Resources* 14, 1160–1170 (2014).

Figures

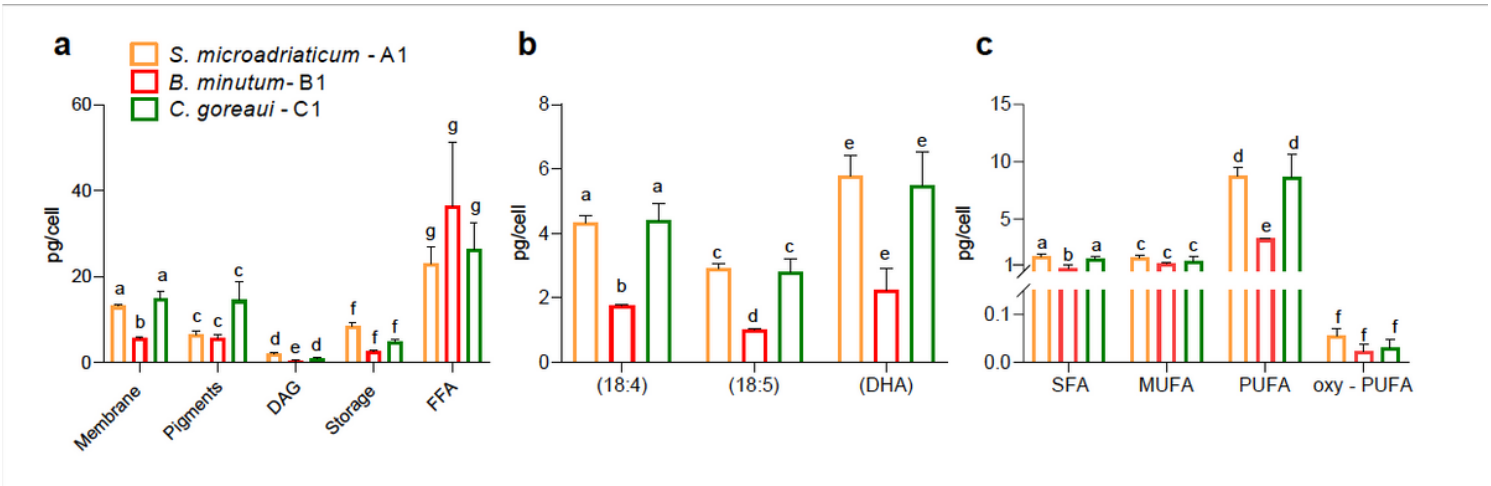

Figure 1

Main lipid classes characterized in Symbiodiniaceae species and saturation index of their membrane lipids growing at baseline (22 ˚C - controls). Mean abundance and their respective standard error bars for (a) the main lipid classes. Membrane lipids (ML) encompass glyco-, phospho-, amino- and sphingo-lipids, plus cardiolipin and cholesterol. Chlorophylls and carotenoids were summed into pigments. Triacylglycerol (TAG) and cholesterol esters (CE) were summed into storage lipids. Diacylglycerol (DAG) and free fatty acids (FFA) were represented separately; (b) shows the main omega-3 (n-3) fatty acids octadecatetraenoic acid, (18:4);octadecapentaenoic acid, (18:5);docosahexaenoic acid, (DHA) and (c) summarizes saturated fatty acids (SFA), monounsaturated fatty acids (MUFA), polyunsaturated fatty acids (PUFA) and oxidized PUFA (oxy-PUFA) that were esterified to ML. Bars with the same letters are not significantly different ($p > 0.01$). Statistical indicators are given in Table S2.

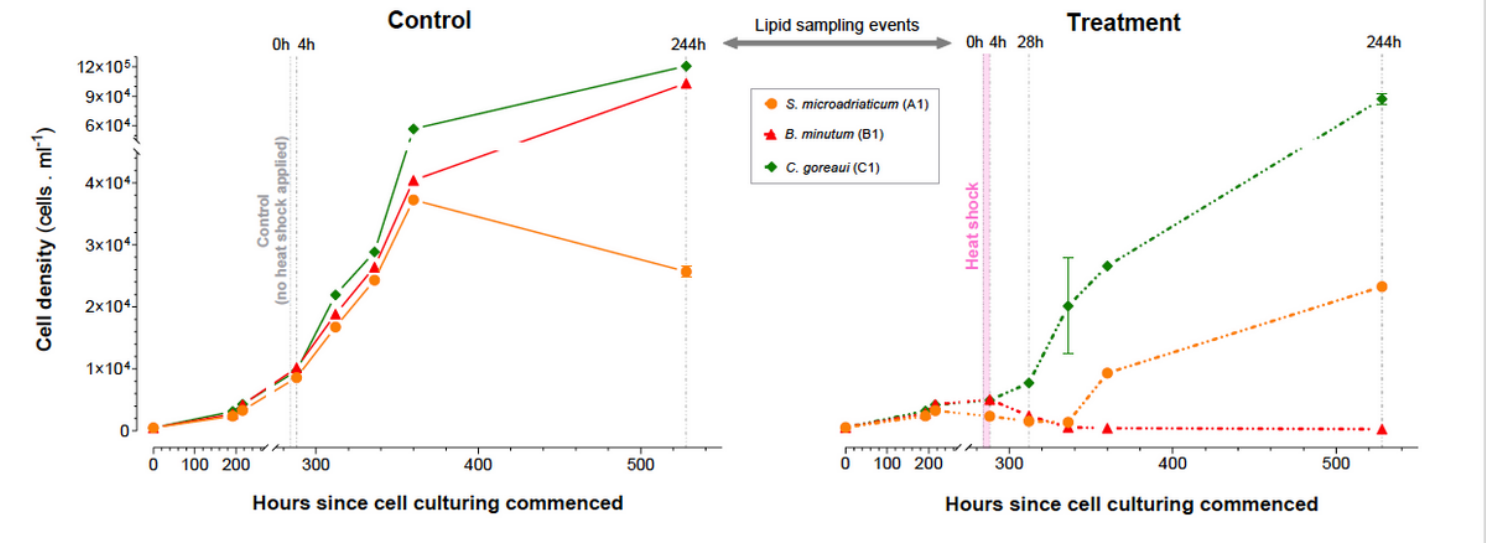

Figure 2

Variation of Symbiodiniaceae population densities since cell culturing commenced. Controls (left) stayed at 22 ˚C throughout the experiment. Heat shock treatment (right) stayed at 34 ˚C for 4 hours after population densities reached exponential growth and were transferred back to 22 ˚C until the end of the experiment. Break in the x and y-axis indicates change in scale to highlight population density data after the heat shock. Vertical lines indicate sampling for lipidomic analysis (i.e., at 0, 4 and 244 hours after the heat shock). Cultures were sampled in triplicates and data is represented as average populational density number with standard errors. Statistical indicators are given in Table S3.

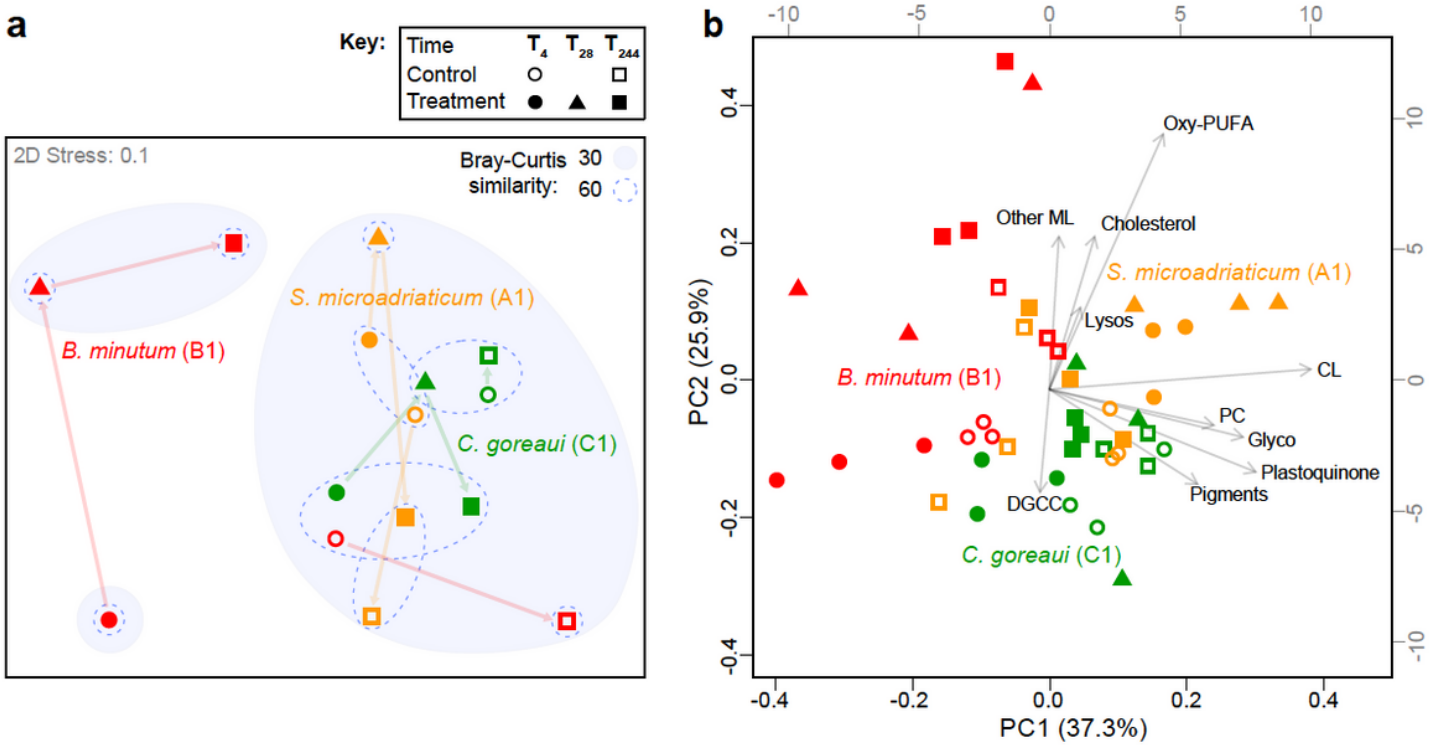

Figure 3

Remodeling of membrane lipids and pigments in Symbiodiniaceae after heat shock. (a) alterations of Symbiodiniaceae membrane lipids, plastoquinone and pigments caused by heat shock. Multidimensional scaling plot (MDS) shows averages of the triplicate experiments of each symbiont (S. microadriaticum – A1 (yellow); B. minutum – B1 (red) and C. goreaui – C1 (green)) at each sampling point for cultures maintained at 22 ˚C (control; i.e., T4 and T244) and exposed to heat shock (treatment; i.e., T4, T28 and T244); (b) principal component analysis (PCA) of membrane lipid classes, pigments and plastoquinone of Symbiodiniaceae species. Total concentration of the sum of all lipid compounds constituing each membrane lipid class (represented in vectors) were used to simplify analysis (cf. Table S1). Lipid classes that were either more abundand or that had polar heads esterified to PUFA and/or PUFA derived products were presented as single vectors, whereas others were gathered as other membrane lipids (Other ML). Abbreviations: PC: phosphatidylcholine; CL: cardiolipin; DGCC: 1,2-diacylglyceryl-3-(O-carboxyhydroxymethylcholine). MGDG: monogalactosyldiacylglycerol; DGDG: digalactosyldiacylglycerol; SQDG: sulfoquinovosyldiacylglycerol and GA: glucoronic acid were grouped as Glycolipids (Glyco). Oxidized PUFA esterified to glycolipids, PC and DGCC were all grouped as Oxy-PUFA. Phosphatidylethanolamine (PE), phosphatidylglycerol (PG), phosphatidylinositol (PI), diacylglyceryltrimethylhomoserine (DGTS) and sphingolipids were grouped as Other ML. Carotenoids and chlorophylls, including chlorophyll-a were grouped as Pigments.

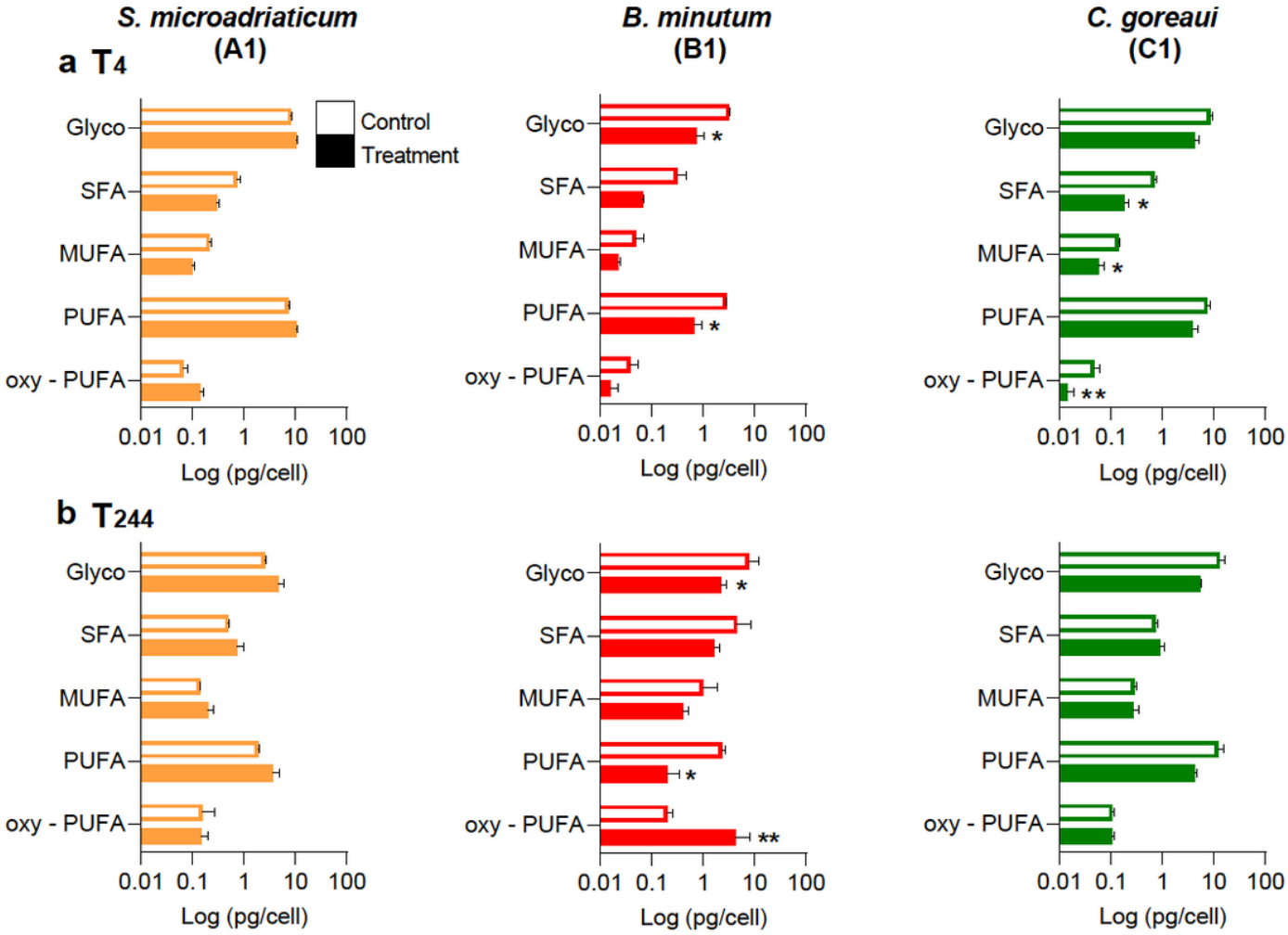

Figure 4

Variation of thylakoid membrane lipids (glycolipids) saturation in Symbiodiniacea after heat shock. Mean abundances of sums of total glycolipids (Glyco), saturared fatty acids (SFA), monounsaturated fatty acids (MUFA), polyunsaturareted fatty acids (PUFA) and oxidized polyunsaturated fatty acids (oxy-PUFA) acyl chains linked to glycolipids normalized in Log10 and their respective standard error bars. Variations at (a) T4 (end of heat shock) and (b) T244 (end of experiment). Graphs show both control (empty bars) and heat shock treatment (filled bars) for each Symbiodiniaceae species (S. microadriaticum – A1 in yellow; B. minutum – B1 in red and C. goreaui – C1 in green). Asterisks (* and **) indicate significant pairwise differences (Tukey's HSD, $p < 0.01$) for Heat shock [Spp.] and Time [Spp.] factors, respectively. Statistical indicators are given in Table S4.

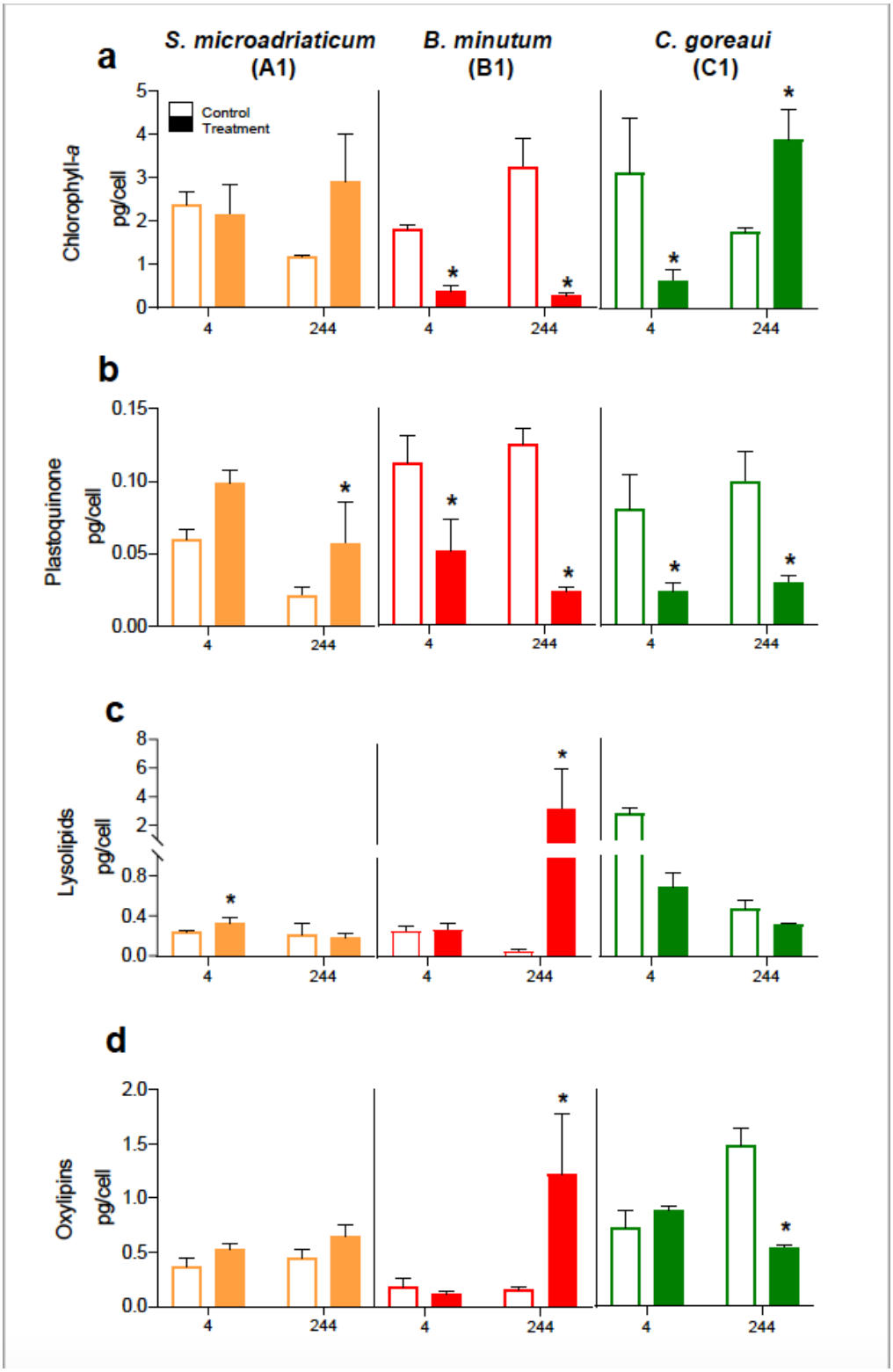

Figure 5

Variation of selected compounds in Symbiodiniaceae after heat shock. Mean abundances in pg/cell and their respective standard error bars of (a) chlorophyll-a, (b) plastoquinone, (c) lysolipids and (d) free oxy-PUFA (oxylipins). Graphs show both control (empty bars) and heat shock treatment (filled bars) for each Symbiodiniaceae species (S. microadriaticum – A1 in yellow; B. minutum – B1 in red and C. goreaui – C1 in green) - at each specific analyzed time T4 (end of heat shock) and T244 (end of experiment). Asterisks

(*) indicate significant pairwise differences (Tukey's HSD, $p < 0.01$) for Heat shock [Spp.] factor. Statistical indicators are given in Table S4.

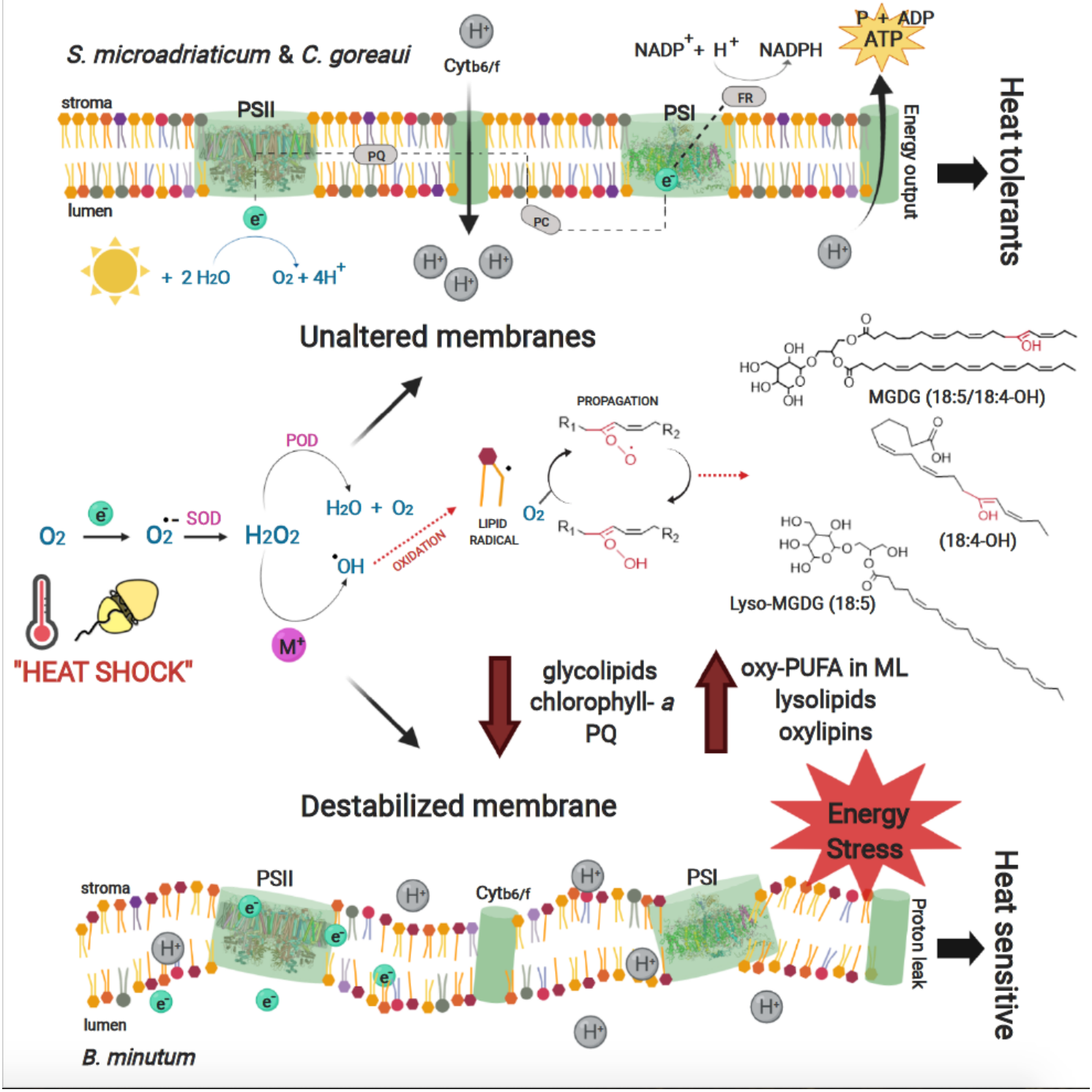

Figure 6

Chemical energy synthesis in thylakoid membranes of Symbiodiniaceae after heat shock. Lipid remodeling of heat tolerant species (upper figure) did not lead to significant variation in specific lipid components of thylakoid membranes, so that S. microadriaticum and C. goreaui had no vital compromise of chemical energy output in the form of adenosine triphosphate (ATP). We propose that

heat can destabilize membranes and unbalance the electron transport chain. The net effect is that excess of high energy electrons may generate free radicals (e.g., hydroxyl •OH) that are likely to oxidize PUFA linked to MLs creating lipid radicals (L• and LOO•) ultimately causing a chain reaction in thylakoid MLs. Such conformational changes in B. minutum (lower figure) may affect the stability of the thylakoid MLs, with potential negative consequences for membrane permeability and ATP output. According to this model, energy output is compromised, cellular growth is impaired and cell death might prevail due to energy stress. Abbreviations: Structural compartments - Cytb6/f = cytochrome b6/f; PSI = Photosystem I. Electron transporters: PQ = plastoquinone; PC = plastocyanin; FR = ferrodoxin. NADPH is the reduced form of nicotinamide adenine dinucleotide phosphate (NADP+); SOD = superoxide dismutase; POD = peroxidase and M+ represents free metal ions (e.g., Fe2+, Cu2+); ML = membrane lipids; MGDG = monogalactosyldiacylglycerol; Oxy-PUFA in ML = oxidized fatty acids esterified to ML.

Supplementary Files

This is a list of supplementary files associated with this preprint. Click to download.

- SupplementaryInformationBotanaetal.docx
- SupplementaryTablesBotanaetal.xlsx
- FigureS1.pdf
- FigureS2.pdf
- FigureS3.pdf
- FigureS4.pdf
- FigureS5.pdf
- FigureS6.pdf